



CXCR4-overexpressed exosomes from cardiosphere-derived cells attenuate myocardial ischemia/reperfusion injury by transferring miRNA to macrophages and regulating macrophage polarization

Yanfeng Ma^{1,2#}, Mingyu Su^{2#}, Wei Qian², Yongli Xuan², Tao Chen², Ran Zhou², Tingbo Jiang^{1*}

¹ Department of Cardiology, The First Affiliated Hospital of Soochow University, Suzhou, Jiangsu 215000, China

² Department of Cardiology, The Affiliated Hospital of Xuzhou Medical University, Xuzhou, Jiangsu 221004, China

ARTICLE INFO

Original paper

Article history:

Received: May 30, 2023

Accepted: August 10, 2023

Published: November 30, 2023

Keywords:

Cardiosphere-derived cells, exosomes, myocardial ischemia/reperfusion injury, CXCR4, M2 macrophage polarization

ABSTRACT

Cardiosphere-derived cells (CDCs) are emerging as ideal candidates for managing cardiac inflammation, albeit with some limitations. Recent literatures have indicated that exosomes secreted by CDCs with C-X-C motif chemokine receptor 4 (CXCR4) overexpression can promote cardiac function after myocardial infarction and there have been some reports of miRNAs involved in ischemia/reperfusion (I/R) therapy. Therefore, we are interested in the role of CXCR4-overexpressed CDC-derived exosomes in delivering specific miRNA after myocardial I/R injury. In this research, we first constructed CDC-derived exosomes that overexpressed CXCR4 and miR-27a-5p, miR-182, or miR-101a. Then, we co-cultured the engineered exosomes with RAW264.7 cells and injected them intravenously into myocardial I/R model mice. In vitro, results showed that proinflammatory cytokines levels in the culture supernatant were decreased and the expression of M2 phenotypic markers were increased. Administration of engineered exosomes improved cardiac function, reduced infarct size, alleviated macrophage infiltration, and regulated M2 macrophage polarization after myocardial I/R, suggesting their implications in cardiac injury repair.

Doi: <http://dx.doi.org/10.14715/cmb/2023.69.12.16>

Copyright: © 2023 by the C.M.B. Association. All rights reserved.

Introduction

Acute myocardial infarction (MI) is a major cause of death and disability worldwide. The preferred treatment strategy for MI patients is timely and effective myocardial reperfusion thrombolytic therapy or direct percutaneous coronary intervention to reduce myocardial ischemia injury and restrict the extent of MI (1). However, cardiac cell death caused by the reperfusion process itself, namely myocardial reperfusion injury, cannot be effectively treated (2, 3). Reperfusion therapy for MI can result in unexpected cardiac complications. After the recovery of blood flow in the infarct area, a variety of inflammatory cells are attracted to the damaged site for tissue repair, in which macrophages are active participants (4). Several studies have shown that altering the polarization status of macrophages can reduce myocardial ischemia/reperfusion (I/R) injury in animal models (5, 6).

The use of cardiosphere-derived cell (CDC) therapy for the treatment of ischemic heart disease has been documented in animals and humans (7, 8). The underlying mechanism of cell therapy remains elusive. Exosomes are nanoscale lipid bilayer vesicles (30-150 nm) secreted by many cell types as a form of local or distal communication between cells. They contain specific amounts of small RNA and protein and are easily absorbed by many cells, including macrophages, fibroblasts, and endothelial cells (9). Recent researches have suggested that exosomes

secreted by mesenchymal stromal cells (MSCs) can boost tissue repair after inflammation and injury in animal models, suggesting that exosomes may contribute to the effect of cell therapy (10-12). It has been shown that genetic engineering that overexpresses C-X-C motif chemokine receptor 4 (CXCR4) enhances the mobilization, implantation, and cardiac repair of MSC in vivo (13). After coronary artery ligation in MI model rats, the administration of MSC-derived CXCR4-overexpressed exosomes preserves cardiac function and enhances MSC-mediated cardioprotection (14). CXCR4-overexpressed exosomes secreted by CDCs have also been reported to confer cardioprotection following I/R injury (15, 16).

MicroRNAs (miRNAs) are short (20-22 nucleotides), noncoding RNAs that are present in exosomes, can be absorbed by neighboring or distant cells, and then regulate the recipient cells (17). The dysregulation of exosomal miRNAs can affect the crosstalk between cancer cells and the tumor microenvironment (18). As reported previously, tumor-derived exosomal miR-934 promotes macrophage M2 polarization to accelerate colorectal cancer metastasis (19). Exosomal miR-500a-5p secreted by cancer-linked fibroblasts accelerates breast cancer cell proliferation (20). The involvement of several miRNAs in myocardial infarction and I/R injury therapy has been reported in numerous studies. MiR-27a-5p attenuates cardiomyocyte injury by regulating autophagy and apoptosis via Atg7 and with its downstream target Ppm1. MiR-27a-5p also modulates

* Corresponding author. Email: jtbsdfyy@163.com

macrophage M2-like polarization (21, 22). MSC-derived exosomes alleviate myocardial I/R injury in mice by delivering miR-182 which regulates macrophage polarization (23). MSC-derived exosomes that contain miR-101a significantly reduce infarct size and improve cardiac function in mice suffering from myocardial I/R (24). In this research, we generated CXCR4-overexpressed exosomes secreted by CDCs and loaded miR-27a-5p, miR-182, or miR-101a into them. We observed a myocardial protective effect of these engineered exosomes in I/R model mice and demonstrated that they improved heart performance by modulating macrophage polarization.

Materials and Methods

Cell Culture

Murine macrophage RAW264.7 cell line was cultured in Dulbecco's modified Eagle's medium (Gibco, USA) supplemented with 10% fetal bovine serum (FBS; Gibco, USA) and 1% penicillin-streptomycin (PS). Human CDCs were cultured in basic Iscove's modified Dulbecco's medium (Lonza, Switzerland) supplemented with 20% FBS and 1% PS. All cells were cultured in an incubator with 5% CO₂ and 95% humidity at 37 °C.

Exosome Isolation and Identification

Exosomes from CDCs were isolated based on a total exosome isolation kit (Invitrogen, USA). The morphology of isolated exosomes was examined using transmission electron microscopy. The concentration and particle size distribution of isolated exosomes were quantified using nanoparticle tracking analysis.

Exosome PKH26 Staining and Cellular Uptake

Isolated exosomes were labeled with PKH26 (Sigma-Aldrich, USA). Briefly, the PKH26 dye was mixed with exosomes and incubated at room temperature. The tagged exosomes were extracted by ultra-centrifugation and cultured with RAW264.7 cells after the staining reaction was stopped. Cells were then fixed with 4% paraformaldehyde (PFA) and stained with 4', 6-diamidino-2-phenylindole (DAPI). The cellular uptake of exosomes was determined using confocal laser microscopy.

Western Blot

Protein was obtained by resuspending the samples in radioimmunoprecipitation assay (RIPA) lysis buffer (Beyotime, China). The concentration was determined using a bicinchoninic acid (BCA) Protein Assay kit (Beyo-

time, China). The protein was subjected to 10% sodium dodecyl-sulfate polyacrylamide gel electrophoresis (SDS-PAGE) and transferred to polyvinylidene fluoride (PVDF) membranes. The membranes were blocked with 1% bovine albumin serum (BSA), and incubated with primary antibodies overnight at 4 °C, and subsequently incubated with secondary antibodies. Antibodies used were as follows: anti-CD63 (Abcam, USA, 1:1000), anti-Alix (Abcam, USA, 1:1000), anti-CD81 (Abcam, USA, 1:1000), CD105 (Abcam, USA, 1:1000), CXCR4 (Abcam, USA, 1:1000), Arg1 (Abcam, USA, 1:1000), INOS (Abcam, USA, 1:1000), β -Actin (Santa Cruz, USA, 1:1000), and Goat Anti-Rabbit IgG H&L (HRP) (Abcam, USA, 1:5000). After staining with enhanced chemiluminescence solution, signals were detected and the expression of certain protein was analyzed using ImageJ analysis software.

Reverse transcription-polymerase chain reaction (RT-PCR)

RNA was extracted using RNAiso Plus reagent (Takara, Japan). The concentration was determined using a NanoDrop 2000 spectrophotometer (Thermo Fisher, USA). Complementary DNA (cDNA) was obtained using a PrimeScript™ RT kit (Takara, Japan) and quantified using an RT-PCR assay labeled with a SYBR Green PCR Mix Kit (Takara, Japan). Results were quantified using the 2- $\Delta\Delta$ CT method. Primers used are listed in Table 1.

Myocardial Ischemia/Reperfusion (I/R)

A thoracotomy at the fourth intercostal space on 8-week male C57BL/6 mice anesthetized with 2% isoflurane was performed. During myocardial I/R surgery, the left anterior descending coronary artery was ligated with a 7-0 silk suture and then released 45 minutes later to allow for reperfusion.

Cardiac Function

A two-dimensional echocardiography was performed using Vevo770 (VisualSonics, Canada) to evaluate cardiac function. Three representative cycles were determined for each mouse, and the left ventricular ejection fraction (LVEF), left ventricular fractional shortening (LVFS), left ventricular end-diastolic volume (LVEDV), as well as with left ventricular end-systolic volume (LVESV) was calculated.

Immunohistochemistry

Mice were perfused intracardially with 4% PFA. Isolated heart tissue was fixed in 4% PFA and then processed

Table 1. Primers used for RT-QPCR.

Target	Forward sequence (5'→3')	Reverse sequence (5'→3')
β -Actin	CATTGCTGACAGGATGCAGAAGG	TGCTGGAAGGTGGACAGTGAGG
Arg1	CATTGGCTTGCAGACGTAGAC	GCTGAAGGTCTCTTCCATCACC
IL-10	CGGGAAGACAATAACTGCACCC	CGGTTAGCAGTATGTTGTCCAGC
CD206	GTTACCTGGAGTGATGGTTCTC	AGGACATGCCAGGGTCACCTTT
TGF β	TGATACGCTGAGTGGCTGTCT	CACAAGAGCAGTGAGCGCTGAA
U6	ATCGGTTGGCAAACGTTTC	TGCGCAGTGGTTTTTGA
miR-27a-5p	GCGGCGGAGGGCTAGCTGCTTG	ATCC AGTGCAGGGTCCGAGG
miR-182	CGTCCTTTGGCAATGGTAGAACTC	GCAGGGTCCGAGGTATTC
miR-101a	TCGTATCCAGTGCAGGGTCCGAGGTG	CACTGGATACGACTCATAACAG

with paraffin embedding. After staining with anti-CD68 (Abcam, USA) overnight at 4 °C, the secondary antibody was applied to evaluate infiltrated macrophages. Confocal microscopy was used to analyze the samples after incubation with DAB solution. Images were processed by ImageJ software.

Statistical analysis

All experiments were performed in triplicate. Data were exhibited as means \pm standard deviation (SD). Statistical analyses were implemented by GraphPad Prism. Between the two groups, a student t-test was used. For three or more groups, a one-way analysis of variance was used. P-value < 0.05 was considered statistically significant.

Results

Construction and characterization of CXCR4-overexpressed CDC-derived exosomes

We first cultured CDCs in vitro and collected exosomes secreted by these cells from the culture media. The morphology of CDC-derived exosomes (CDC-Exo) was examined using transmission electron microscopy (TEM) (Figure 1A). Purified CDC-Exo presented a round-shaped vesicular membrane structure. The concentration and particle size distribution of CDC-Exo within the culture media were analyzed by nanoparticle tracking analysis (Figure 1B). For CDC-Exo characterization, we performed a western blot to detect three typical exosome markers (CD63, CD81, and Alix) and a CDC surface marker CD105 (Figure 1C). Then, we obtained CXCR4-overexpressed exosomes (CXCR4-Exo) by transfecting CXCR4-overexpressing plasmids in CDCs. Exosomes secreted by CDCs transfected with empty plasmids were used as a control. Flow cytometry as well as western blot demonstrated that CXCR4 could be examined on the CXCR4-Exo (Figure 1D, E).

Uptake of CXCR4-Exo by macrophages

After the successful construction of CXCR4-Exo, we investigated the internalization of these engineered exo-

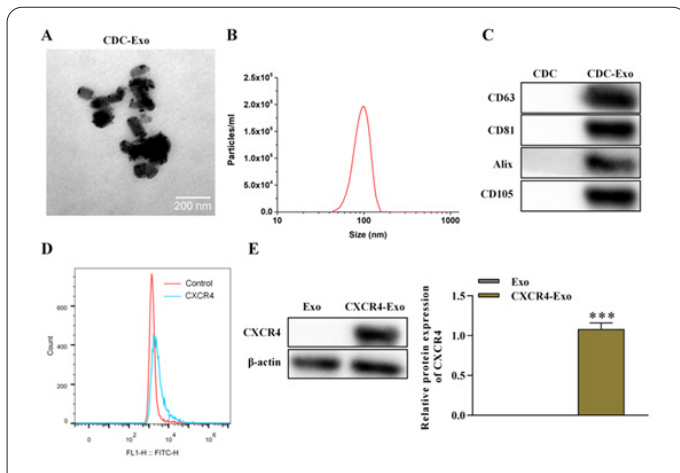


Figure 1. Identification of CDC-Exo and CXCR4 expression. (A) CDC-Exo morphology observed by TEM. Scale bars, 200 nm. (B) Concentration and particle size distribution were measured by nanoparticle tracking analysis. (C) Quantification of CDC-Exo surface markers by Western blot. (D) Exosomal CXCR4 expression was detected by flow cytometry. (E) Exosomal CXCR4 expression was quantified by Western blot. N=5, ***p < 0.001.

somes by RAW264.7 cells. We pre-treated exosomes with PKH26, a lipophilic dye that stained the lipid membrane of exosome vesicles. PKH26-labeled exosomes were cultured with RAW264.7 cells and the confocal laser microscopy revealed the presence of PKH26-positive RAW264.7 cells in both the Exo group and the CXCR4-Exo group (Figure 2A). The CXCR4 expression in RAW264.7 cells was measured by flow cytometry. After co-culture with CXCR4-Exo, the CXCR4 fluorescent signals of RAW264.7 cells were more intense (Figure 2B), indicating that these cells had successfully taken up CXCR4-Exo.

Engineered exosomes modulated the polarization of macrophages to M2 phenotype

Based on CXCR4 overexpression, we generated overexpressed DC-exosomes of miR-27a-5p, miR-182, or miR-101a by electroporation, and we confirmed the efficacy of exogenous miRNA transfection by RT-PCR (Figure 3A). RAW264.7 cells were activated with lipopolysaccharide (LPS) and the engineered exosomes or Exo-NC was added to the medium 6 h later. Compared with Exo-NC co-cultured cells, the expression of miR-27a-5p, miR-182, and miR-101a was increased in cells co-cultured with Exo-miR after 48 h (Figure 3B).

Enzyme-linked immunosorbent assay (ELISA) was adopted to measure the levels of pro-inflammatory cytokine IL-6 and anti-inflammatory cytokine IL-10 in the supernatant. We discovered that Exo-miR reduced LPS-

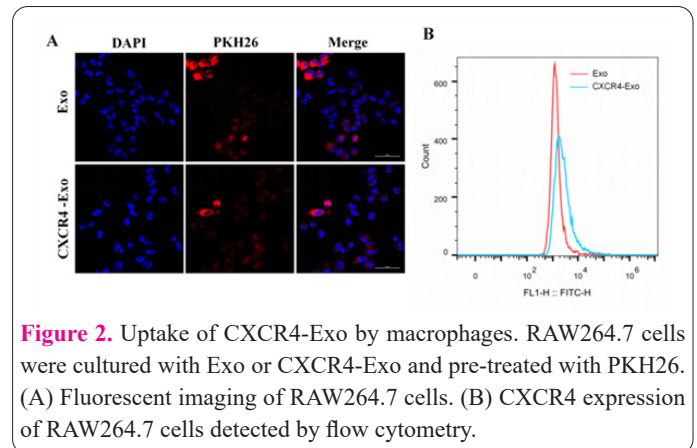


Figure 2. Uptake of CXCR4-Exo by macrophages. RAW264.7 cells were cultured with Exo or CXCR4-Exo and pre-treated with PKH26. (A) Fluorescent imaging of RAW264.7 cells. (B) CXCR4 expression of RAW264.7 cells detected by flow cytometry.

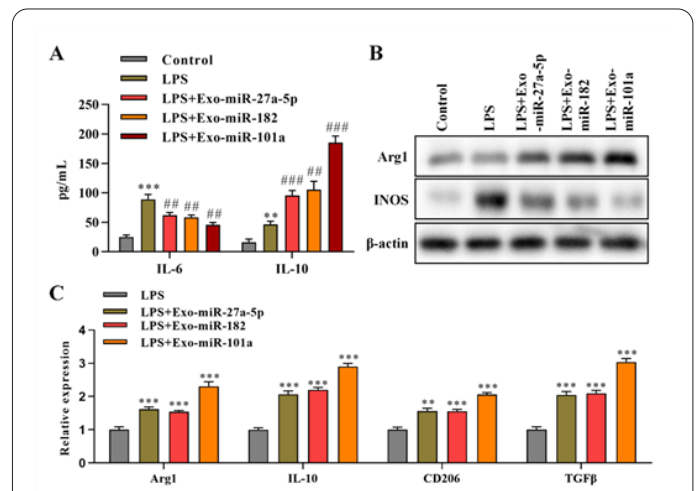


Figure 3. Verification of miRNA transfection into CXCR4-Exo and macrophage uptake. (A) RT-PCR examined the efficiency of miRNA transfer into exosomes. (B) RT-PCR analysis of the miRNA expression in RAW264.7 cells after co-culture for 48 h. N=5, ***p < 0.001.

induced IL-6 production and enhanced the secretion of IL-10, with Exo-miR-101a causing the most notable change (Figure 4A). Western blot analysis was used to assess the expression of the M1 and M2 macrophage markers INOS and Arg1, respectively. In comparison to the LPS group, the expression of INOS in three miR-Exo groups was down-regulated, and the expression of Arg1 was up-regulated (Figure 4B), indicating that M2 macrophages were more than M1 macrophages. By using RT-PCR, we also measured the M2 macrophage marker and anti-inflammatory cytokine expression levels. We found that the expression of Arg1, CD206, IL-10, and TGF- β was elevated by Exo-miR (Figure 4C). These findings showed that M1 macrophages could be converted in vitro into M2 macrophages by engineered exosomes.

Engineered exosomes improved cardiac performance following myocardial ischemia/reperfusion injury

To determine the therapeutic effect of engineered exosomes in vivo, Exo-miR or Exo-NC was injected intravenously after myocardial ischemia/reperfusion (I/R) injury. Echocardiography was performed to detect cardiac function and tissue was collected for histological examination. Exo-miR administration significantly reduced left ventricle dilation caused by I/R (Figure 5A). When compared to the Exo-NC group, Exo-miR treatment dramatically decreased LVEDV and LVESV and increased LVEF and LVFS (Figure 5B). The infarct size and the collagen area of the hearts were next evaluated. Masson trichrome staining showed that the infarct size of the three Exo-miR groups was significantly smaller, and the reduction of the infarct size of the Exo-miR-101a group was the largest (Figure 5C). Sirius Red staining revealed that all therapeutic groups experienced a substantial decrease in collagen area (Figure 5D). Together, these findings indicated that engineered exosomes could significantly enhance heart function following I/R injury.

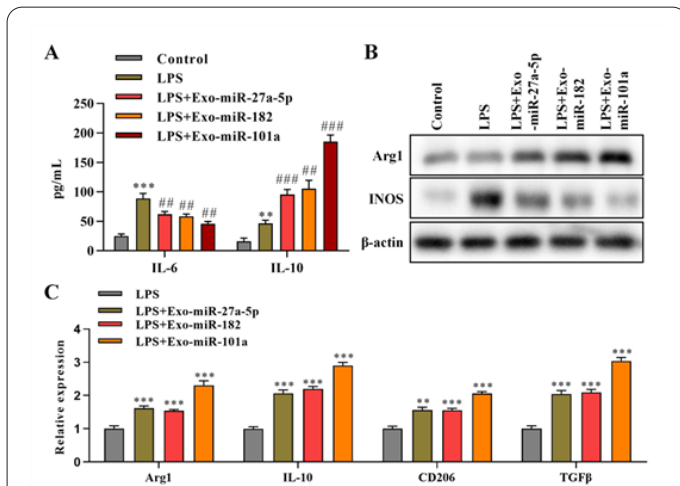


Figure 4. Exo-miR regulated the macrophage polarization to M2 phenotype in response to LPS stimulation. LPS was used to activate RAW264.7 cells for 6 h before co-culturing cells with Exo-miR-27a-5p, Exo-miR-182, and Exo-miR-101a for 48 h. (A) The concentration of IL-6 and IL-10 in the supernatant was measured by ELISA. N=5, **p < 0.01, ***p < 0.001 compared with control. ##p < 0.01, ###p < 0.001 compared with LPS. (B) Western blot showing the expression of INOS and Arg1 in RAW 264.7 cells. (C) Quantification of Arg1, IL-10, CD206, and TGF β expression of RAW 264.7 cells by RT-PCR. N=5, **p < 0.01, ***p < 0.001.

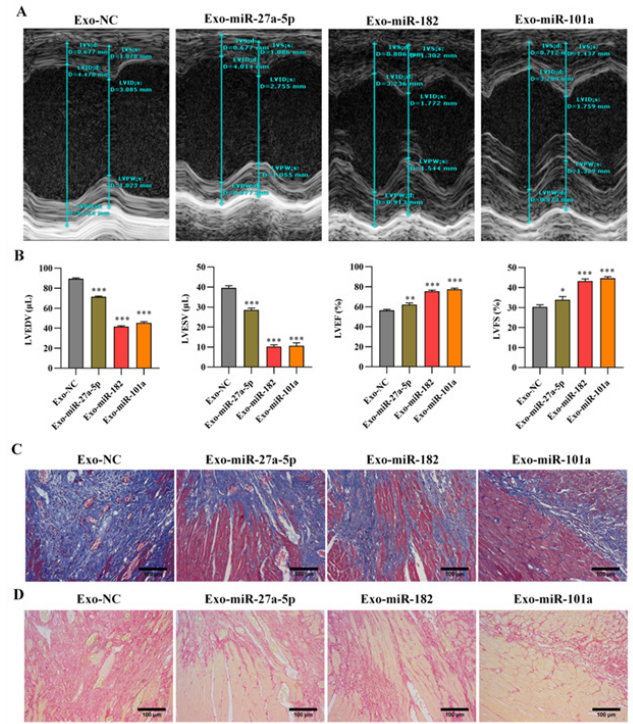


Figure 5. Engineered exosomes enhanced cardiac function following myocardial I/R injury. Exo-miR or Exo-NC was injected intravenously after myocardial I/R injury. (A) Representative echocardiogram of mouse hearts after exosome administration. (B) LVEDV, LVESV, LVEF, and LVFS in mice intravenously injected exosomes. N=5, *p < 0.05, **p < 0.01, ***p < 0.001. (C) Masson trichrome staining of transverse heart sections showing infarct region. (D) Sirius Red staining images showing collagen area.

Engineered exosomes reduced macrophage infiltration and promoted M2 macrophage polarization in vivo

Engineered exosomes have been shown to have therapeutic effects on I/R model mice, and we speculated it was connected to the status of macrophages. Immunohistochemistry and flow cytometry were employed to identify heart-infiltrating macrophages after myocardial I/R injury. Macrophage infiltration was decreased significantly in the three Exo-miR groups (Figure 6A, B). Next, we isolated cardiac macrophages from mice treated with either Exo-miR or Exo-NC and measured the expression levels of macrophage phenotype markers. Results from RT-PCR revealed that Arg1, IL-10, CD206, and TGF were all up-regulated in Exo-miR treatment group (Figure 6C).

Discussion

Currently, in the treatment of acute myocardial infarction (MI), surgery and drug therapy are mainly used to restore myocardial perfusion. Even if blood flow is restored rapidly, the phenomenon of myocardial reperfusion injury may still occur. Ischemia/reperfusion (I/R) initiates a chain of events that leads to inflammation of the heart (25). Myocardial ischemic infarction and scar formation are closely related to the duration and intensity of these inflammatory processes. Macrophages, along with other inflammatory cells, are crucial in the modulation of cardiac inflammation (26). Macrophages are composed of different subtypes. They provide powerful pro-inflammatory signals to injured cardiomyocytes and repair clues to

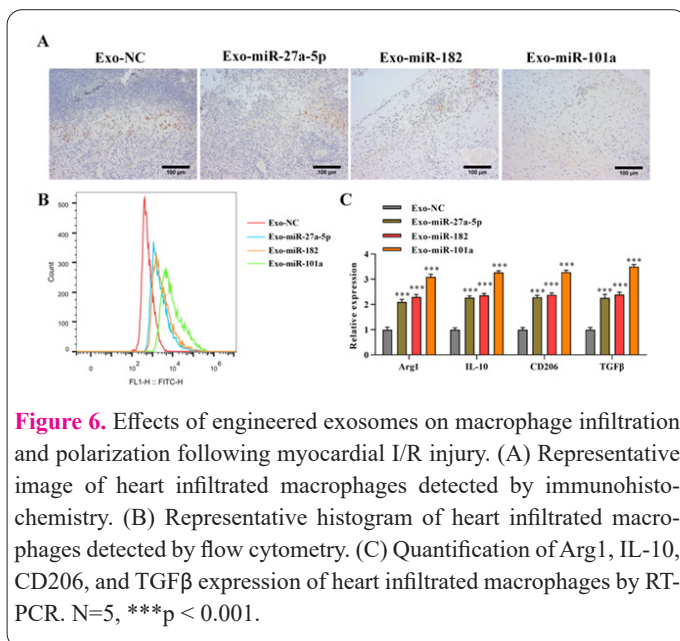


Figure 6. Effects of engineered exosomes on macrophage infiltration and polarization following myocardial I/R injury. (A) Representative image of heart infiltrated macrophages detected by immunohistochemistry. (B) Representative histogram of heart infiltrated macrophages detected by flow cytometry. (C) Quantification of Arg1, IL-10, CD206, and TGFβ expression of heart infiltrated macrophages by RT-PCR. N=5, ***p < 0.001.

tissue healing (27). In animal models, changing the polarization status of macrophages can attenuate cardiac I/R injury (5, 6), indicating that macrophage polarization is a potent therapeutic target for MI.

Currently, the benefit of CDC therapy in myocardial ischemic injury has been proven in animal and clinical studies (7, 8). The positive effects of cell treatment are long-lasting, but there are also some drawbacks such as limited cardiac retention (28). It has been reported that exosomes secreted by CDCs reduce scarring and improve heart function in porcine myocardial infarction (29). CXCL12 is a member of the CXC chemokine family, and its expression is upregulated in the infarcted myocardium due to the activation of hypoxia-inducible factor-1 (HIF-1) (30). Studies have shown that the plasma level of CXCL12 is elevated in patients after MI, and CXCL12 recruits CXCR4-expressing cells, including circulating progenitor cells by binding CXCR4 (31). The function of CXCL12 to attract circulating progenitor cells into infarcted areas facilitates tissue repair. Ciullo A, et al have reported that overexpressing CXCR4 enhances the bioavailability of cardioprotective CDC-derived exosomes to ischemic hearts (32).

The relationship between miRNAs and myocardial infarction and I/R injury has been extensively studied in recent years. For instance, miR-22 is increased in I/R model rats and inhibits miR-22 and reduces the damage induced by I/R. In addition, an increased level of miR-22 in vitro exacerbates oxidative stress and mitochondrial damage carried on by I/R (33). By lowering oxidative stress and decreasing ROS, miR-126 overexpression repairs endothelial progenitor cell injury (34). In rat ventricular cardiomyocytes, miR-145 dramatically downregulates CaMKII levels, inhibits calcium overload caused by hydrogen peroxide, and reduces the production of ROS. MiR-145 protects cardiomyocytes subjected to oxidative stress and the hearts of I/R model mice (35, 36). MiR-340-5p overexpression suppresses ROS and MDA levels and restores cell viability of cardiomyocytes impaired by I/R (37-39).

In this study, we generated and identified CXCR4-overexpressed exosomes from CDCs (CXCR4-Exo) and demonstrated its normal cellular internalization by RAW264.7 cells. Then, we loaded CXCR4-Exo with miR-27a-5p, miR-182, or miR-101a, whose myocardial

protective functions have been reported following I/R injury. These engineered exosomes were added into the RAW264.7 cell culture media to regulate cell polarization. Next, we intravenously injected the engineered exosomes into myocardial I/R model mice and observed significant improvements in cardiac function and infarct size compared to Exo-NC. The myocardial protection was achieved by inhibiting macrophage infiltration and boosting M2 phenotype polarization. Our study combined CDC-derived exosomes, CXCR4 genetic modification, and miRNA treatment. This approach may represent as an alternative promising strategy for alleviating ischemic coronary syndromes.

Conclusions

In conclusion, our study demonstrated that CXCR4-overexpressed exosomes from cardiosphere-derived cells attenuated myocardial ischemia/reperfusion injury by transferring miRNA to macrophages and regulating macrophage polarization, which might provide a promising target for the treatment of myocardial ischemia/reperfusion injury.

Acknowledgements

Not applicable.

Interest conflict

The authors state that there are no conflicts of interest.

Consent for publications

Not applicable.

Availability of data and material

All data generated during this study are included in this published article

Authors' Contribution

TBJ conceived and designed the study. YFM and MYS conducted most of the experiments. WQ and YLX analyzed the data. TC and RZ performed the literature search and data extraction. YFM and MYS drafted the manuscript. TBJ finalized the manuscript. All authors read and approved the final manuscript.

Funding

Not applicable.

Ethics approval and consent to participate

All animal experiments should comply with the ARRIVE guidelines. The experimental protocol was approved by the Animal Ethics Committee of Soochow University.

References

- Gao RL, Han YL, Yang XC, et al. Thrombolytic therapy with rescue percutaneous coronary intervention versus primary percutaneous coronary intervention in patients with acute myocardial infarction: a multicenter randomized clinical trial. *Chin Med J (Engl)* 2010; 123(11):1365-72.
- Huang CK, Dai D, Xie H, et al. Lgr4 Governs a Pro-Inflammatory Program in Macrophages to Antagonize Post-Infarction Cardiac Repair. *Circ Res* 2020; 127(8):953-73.
- Hausenloy DJ, Yellon DM. Myocardial ischemia-reperfusion injury: a neglected therapeutic target. *J Clin Invest* 2013; 123(1):92-

- 100.
4. Zhang S, Bories G, Lantz C, et al. Immunometabolism of Phagocytes and Relationships to Cardiac Repair. *Front Cardiovasc Med* 2019; 6:42.
 5. Kim Y, Nurakhayev S, Nurkesh A, Zharkinbekov Z, Saparov A. Macrophage Polarization in Cardiac Tissue Repair Following Myocardial Infarction. *Int J Mol Sci* 2021; 22(5).
 6. Mouton AJ, DeLeon-Pennell KY, Rivera Gonzalez OJ, et al. Mapping macrophage polarization over the myocardial infarction time continuum. *Basic Res Cardiol* 2018; 113(4):26.
 7. Ostovaneh MR, Makkar RR, Ambale-Venkatesh B, et al. Effect of cardiosphere-derived cells on segmental myocardial function after myocardial infarction: ALLSTAR randomised clinical trial. *Open Heart* 2021; 8(2):e001614.
 8. Cheng K, Malliaras K, Smith RR, et al. Human cardiosphere-derived cells from advanced heart failure patients exhibit augmented functional potency in myocardial repair. *JACC Heart Fail* 2014; 2(1):49-61.
 9. Kalluri R, LeBleu VS. The biology, function, and biomedical applications of exosomes. *Science* 2020; 367(6478):eaau6977.
 10. Zhang S, Chuah SJ, Lai RC, et al. MSC exosomes mediate cartilage repair by enhancing proliferation, attenuating apoptosis and modulating immune reactivity. *Biomaterials* 2018; 156:16-27.
 11. Aliotta JM, Pereira M, Wen S, et al. Exosomes induce and reverse monocrotaline-induced pulmonary hypertension in mice. *Cardiovasc Res* 2016; 110(3):319-30.
 12. Xiao C, Wang K, Xu Y, et al. Transplanted Mesenchymal Stem Cells Reduce Autophagic Flux in Infarcted Hearts via the Exosomal Transfer of miR-125b. *Circ Res* 2018; 123(5):564-78.
 13. Wu SZ, Li YL, Huang W, et al. Paracrine effect of CXCR4-overexpressing mesenchymal stem cells on ischemic heart injury. *Cell Biochem Funct* 2017; 35(2):113-23.
 14. Kang K, Ma R, Cai W, et al. Exosomes Secreted from CXCR4 Overexpressing Mesenchymal Stem Cells Promote Cardioprotection via Akt Signaling Pathway following Myocardial Infarction. *Stem Cells Int* 2015; 2015:659890.
 15. Rezaie J, Rahbarghazi R, Pezeshki M, et al. Cardioprotective role of extracellular vesicles: a highlight on exosome beneficial effects in cardiovascular diseases. *J Cell Physiol* 2019; 234(12):21732-45.
 16. Pan W, Zhu Y, Meng X, et al. Immunomodulation by exosomes in myocardial infarction. *J Cardiovasc Transl Res* 2019; 12(1):28-36.
 17. Mori MA, Ludwig RG, Garcia-Martin R, Brandão BB, Kahn CR. Extracellular miRNAs: From Biomarkers to Mediators of Physiology and Disease. *Cell Metab* 2019; 30(4):656-73.
 18. Tan S, Xia L, Yi P, et al. Exosomal miRNAs in tumor microenvironment. *J Exp Clin Cancer Res* 2020; 39(1):67.
 19. Zhao S, Mi Y, Guan B, et al. Tumor-derived exosomal miR-934 induces macrophage M2 polarization to promote liver metastasis of colorectal cancer. *J Hematol Oncol* 2020; 13(1):156.
 20. Chen B, Sang Y, Song X, et al. Exosomal miR-500a-5p derived from cancer-associated fibroblasts promotes breast cancer cell proliferation and metastasis through targeting USP28. *Theranostics* 2021; 11(8):3932-47.
 21. Goto S, Ichihara G, Katsumata Y, et al. Time-Series Transcriptome Analysis Reveals the miR-27a-5p-Ppm1l Axis as a New Pathway Regulating Macrophage Alternative Polarization After Myocardial Infarction. *Circ J* 2021; 85(6):929-38.
 22. Zhang J, Qiu W, Ma J, et al. miR-27a-5p Attenuates Hypoxia-induced Rat Cardiomyocyte Injury by Inhibiting Atg7. *Int J Mol Sci* 2019; 20(10).
 23. Zhao J, Li X, Hu J, et al. Mesenchymal stromal cell-derived exosomes attenuate myocardial ischaemia-reperfusion injury through miR-182-regulated macrophage polarization. *Cardiovasc Res* 2019; 115:1205 - 16.
 24. Wang J, Lee CJ, Deci MB, et al. MiR-101a loaded extracellular nanovesicles as bioactive carriers for cardiac repair. *Nanomedicine* 2020; 27:102201.
 25. Ong SB, Hernández-Reséndiz S, Crespo-Avilan GE, et al. Inflammation following acute myocardial infarction: Multiple players, dynamic roles, and novel therapeutic opportunities. *Pharmacol Ther* 2018; 186:73-87.
 26. Liu J, Wang H, Li J. Inflammation and Inflammatory Cells in Myocardial Infarction and Reperfusion Injury: A Double-Edged Sword. *Clin Med Insights Cardiol* 2016; 10:79-84.
 27. Hulsmans M, Sam F, Nahrendorf M. Monocyte and macrophage contributions to cardiac remodeling. *J Mol Cell Cardiol* 2016; 93:149-55.
 28. Malliaras K, Ibrahim A, Tseliou E, et al. Stimulation of endogenous cardioblasts by exogenous cell therapy after myocardial infarction. *EMBO Mol Med* 2014; 6(6):760-77.
 29. Gallet R, Dawkins J, Valle J, et al. Exosomes secreted by cardiosphere-derived cells reduce scarring, attenuate adverse remodeling, and improve function in acute and chronic porcine myocardial infarction. *Eur Heart J* 2017; 38(3):201-11.
 30. Penn MS. Importance of the SDF-1: CXCR4 axis in myocardial repair. *Circ Res* 2009; 104(10):1133-5.
 31. Ziff OJ, Bromage DI, Yellon DM, Davidson SM. Therapeutic strategies utilizing SDF-1 α in ischaemic cardiomyopathy. *Cardiovasc Res* 2017; 114(3):358-67.
 32. Ciullo A, Biemmi V, Milano G, et al. Exosomal Expression of CXCR4 Targets Cardioprotective Vesicles to Myocardial Infarction and Improves Outcome after Systemic Administration. *Int J Mol Sci* 2019; 20(3).
 33. Du JK, Cong BH, Yu Q, et al. Upregulation of microRNA-22 contributes to myocardial ischemia-reperfusion injury by interfering with the mitochondrial function. *Free Radic Biol Med* 2016; 96:406-17.
 34. Pan Q, Zheng J, Du D, et al. MicroRNA-126 Priming Enhances Functions of Endothelial Progenitor Cells under Physiological and Hypoxic Conditions and Their Therapeutic Efficacy in Cerebral Ischemic Damage. *Stem Cells Int* 2018; 2018:2912347.
 35. Liu Z, Tao B, Fan S, et al. MicroRNA-145 Protects against Myocardial Ischemia Reperfusion Injury via CaMKII-Mediated Antiapoptotic and Anti-Inflammatory Pathways. *Oxid Med Cell Longev* 2019; 2019:8948657.
 36. Cha M-J, Jang J-K, Ham O, et al. MicroRNA-145 suppresses ROS-induced Ca²⁺ overload of cardiomyocytes by targeting CaMKII δ . *Biochemical and Biophysical Research Communications* 2013; 435(4):720-6.
 37. Zhang C, Zeng L, Cai G, et al. miR-340-5p Alleviates Oxidative Stress Injury by Targeting MyD88 in Sepsis-Induced Cardiomyopathy. *Oxid Med Cell Longev* 2022; 2022:2939279.
 38. Kakaei M, Rehman FU, Fazeli F. The effect of chickpeas metabolites on human diseases and the application of their valuable nutritional compounds suitable for human consumption. *Cell Mol Biomed Rep* 2024; 4(1): 30-42. doi: 10.55705/cembr.2023.395591.1153.
 39. Li D, Zhou J, Yang B, Yu Y. microRNA-340-5p inhibits hypoxia/reoxygenation-induced apoptosis and oxidative stress in cardiomyocytes by regulating the Act1/NF- κ B pathway. *J Cell Biochem* 2019; 120(9):14618-27.